

## General Disclaimer

### One or more of the Following Statements may affect this Document

- This document has been reproduced from the best copy furnished by the organizational source. It is being released in the interest of making available as much information as possible.
- This document may contain data, which exceeds the sheet parameters. It was furnished in this condition by the organizational source and is the best copy available.
- This document may contain tone-on-tone or color graphs, charts and/or pictures, which have been reproduced in black and white.
- This document is paginated as submitted by the original source.
- Portions of this document are not fully legible due to the historical nature of some of the material. However, it is the best reproduction available from the original submission.

(NASA-CR-158570) LASER-ZONE GROWTH IN A  
RIBBON-TO-RIBBON (RTR) PROCESS SILICON SHEET  
GROWTH DEVELOPMENT FOR THE LARGE AREA  
SILICON SHEET TASK OF THE LOW COST SOLAR  
ARRAY PROJECT Technical (Motorola, Inc.)

N79-24473

Unclas  
25190

G3/44

LASER-ZONE GROWTH IN A RIBBON-TO-RIBBON (RTR) PROCESS  
SILICON SHEET GROWTH DEVELOPMENT FOR THE LARGE AREA  
SILICON SHEET TASK OF THE LOW COST SOLAR ARRAY PROJECT

TECHNICAL QUARTERLY REPORT NO. 10

MOTOROLA REPORT NO. 2256/13

1 JANUARY 1979 - 31 MARCH 1979

JPL CONTRACT NO. 954376

BY

A. BAGHDADI, R. W. GURTLER, R. LEGGE,  
B. SOPORI, M. J. RICE, R. J. ELLIS

PREPARED BY

MOTOROLA INC.

SEMICONDUCTOR GROUP

5005 EAST McDOWELL ROAD

PHOENIX, ARIZONA 850085



THE JPL LOW-COST SOLAR ARRAY PROJECT IS SPONSORED BY THE U.S. DEPARTMENT OF ENERGY AND FORMS PART OF THE SOLAR PHOTOVOLTAIC CONVERSION PROGRAM TO INITIATE A MAJOR EFFORT TOWARD THE DEVELOPMENT OF LOW-COST SOLAR ARRAYS. THIS WORK WAS PERFORMED FOR THE JET PROPULSION LABORATORY, CALIFORNIA INSTITUTE OF TECHNOLOGY BY AGREEMENT BETWEEN NASA AND DOE.

MOTOROLA PROJECT NO's 2319 - 25

LASER-ZONE GROWTH IN A RIBBON-TO-RIBBON (RTR) PROCESS  
SILICON SHEET GROWTH DEVELOPMENT FOR THE LARGE AREA  
SILICON SHEET TASK OF THE LOW COST SOLAR ARRAY PROJECT

TECHNICAL QUARTERLY REPORT NO. 10

MOTOROLA REPORT NO. 2256/13

1 JANUARY 1979 - 31 MARCH 1979

JPL CONTRACT NO. 954376

BY

A. BAGHDADI, R. W. GURTLER, R. LEGGE,  
B. SOPORI, M. J. RICE, R. J. ELLIS

PREPARED BY

MOTOROLA INC.

SEMICONDUCTOR GROUP

5005 EAST McDOWELL ROAD

PHOENIX, ARIZONA 850085

THE JPL LOW-COST SOLAR ARRAY PROJECT IS SPONSORED BY THE U.S. DEPARTMENT OF ENERGY AND FORMS PART OF THE SOLAR PHOTOVOLTAIC CONVERSION PROGRAM TO INITIATE A MAJOR EFFORT TOWARD THE DEVELOPMENT OF LOW-COST SOLAR ARRAYS. THIS WORK WAS PERFORMED FOR THE JET PROPULSION LABORATORY, CALIFORNIA INSTITUTE OF TECHNOLOGY BY AGREEMENT BETWEEN NASA AND DOE.

THIS REPORT WAS PREPARED AS AN ACCOUNT OF WORK SPONSORED BY THE UNITED STATES GOVERNMENT. NEITHER THE UNITED STATES NOR THE UNITED STATES DEPARTMENT OF ENERGY, NOR ANY OF THEIR EMPLOYEES, MAKES ANY WARRANTY, EXPRESS OR IMPLIED, OR ASSUMES ANY LEGAL LIABILITY OR RESPONSIBILITY FOR THE ACCURACY, COMPLETENESS OR USEFULNESS OF ANY INFORMATION, APPARATUS, PRODUCT OR PROCESS DISCLOSED, OR REPRESENTS THAT ITS USE WOULD NOT INFRINGE PRIVATELY OWNED RIGHTS.

## TABLE OF CONTENTS

<u>SECTION</u>	<u>TITLE</u>	<u>PAGE</u>
1.0	Crystal Growth Using The Purgeable Furnace	1
2.0	Polycrystalline Ribbon Development	4
2.1	Substrate Studies - Multilayer Systems	6
3.0	Neutron Activation Analysis	7
4.0	Diffusion Length Measurements By SPV, OCPV	9
5.0	Solar Cells On Gettered Silicon Ribbons	13
5.1	Metallization Shadowing	13
5.2	Variation In Short-Circuit Current	13
5.3	Metallization Sintering	16
5.4	Cells On Ribbons Grown In The Purgeable Furnace	16
5.5	Large Area Solar Cells	18
6.0	Preliminary Results Of Infrared Absorption Measurements	18
7.0	Problems	22
8.0	Plans	23
9.0	New Technology	23
10.0	Program Milestones	24

## SUMMARY

This quarter has witnessed appreciable progress in achieving high efficiency on RTR solar cells, with an average efficiency of 9.1% on the most recent lot. The best cell to date has a measured efficiency of 11.3%.

A new technique for growing limited-length ribbons continually has been demonstrated. This "Rigid Edge" technique can be used to recrystallize about 95% of the polyribbon feedstock. A major advantage of this method is that only a single, constant length silicon ribbon is handled throughout the entire process sequence; this may be accomplished using cassettes similar to those presently in use for processing Czochralski wafers. Thus a transition from Cz to ribbon technology can be smoothly affected. The maximum size being considered, 3" x 24", is half a square foot, and will generate 6 watts for 12% efficiency at 1 sun.

Silicon dioxide has been demonstrated as an effective, practical diffusion barrier for use during the polyribbon formation. Two different approaches for using the silicon dioxide are being pursued.

## LIST OF FIGURES

<u>NUMBER</u>	<u>TITLE</u>	<u>PAGE</u>
1	Grain Structure At The Edge, Rigid Edge Method	2
2	Grain Structure At The Center, Rigid Edge Method	2
3	Grain Structure, Full Width Melt	2
4	Entrance Seal, CVD Furnace	5
5	SiO <sub>2</sub> Diffusion Barrier - Cross-Section	8
6	Diffusion Length Measurements On Inhomogeneous Material	12
7	I-V Curve, High Efficiency Cell	14
8	Correlation Of Short-Circuit Current Density And Diffusion Length	17
9	6 x 4 cm <sup>2</sup> Cell	19
10	Behavior Of Oxygen In RTR Silicon Ribbons Grown From Various Feedstock Types	20
11	Dependence Of I On Net Oxygen and Oxygen Complexes	21

LIST OF TABLES

<u>NUMBER</u>	<u>TITLE</u>	<u>PAGE</u>
I	Neutron Activation Analysis	10
II	RTR Cells Fabricated On Pre-Etched CVD Feedstock	15



## 1.0 CRYSTAL GROWTH USING THE PURGEABLE FURNACE

Recent modifications to the purgeable furnace have apparently succeeded in reducing (or eliminating) contamination of the silicon ribbon during growth. (See Section 5.4) The quartz jacket was rebuilt, with its flanges sloping up at a  $10^\circ$  angle, to prevent reflected beams from striking it during growth. This change allowed removal of the protective platinum shields, which may have been the contamination source. Gas flow between the pre- and post-heaters has been restricted by stuffing the gap with high purity quartz wool. This has effectively increased the outward gas flow around the melt, thus further improving ambient control. The quartz wool has also proved beneficial in stabilizing the temperature in the heaters.

Ribbons grown from pre-etched CVD feedstock in this furnace were fabricated into solar cells. Results for the best cells are quoted in Section 5.4.

The ribbons were grown at 1"/minute using the rigid edge technique. In the rigid edge technique, the molten zone is not allowed to touch the ribbon edges. Since the ribbon is supported by the solid edges, it does not need to be held at both the top and the bottom. By holding ribbons from the top only, and growing to within 1/8" from the bottom of the ribbon, we were able to grow approximately  $45 \text{ cm}^2/\text{ribbon}$ . If we had to hold the ribbon at both top and bottom, the total regrown length would have only been  $\sim 7 \text{ cm}$ ; thus the total area grown would have been restricted to  $\sim 17 \text{ cm}^2$ .

Grain structure of ribbons grown by this technique is remarkably similar to that of ribbons grown from a full-width melt. Naturally, nucleation from the edge does occur (Figure 1) but the edge-influenced grain growth extends only  $\sim 1 \text{ mm}$  into the ribbon. Across most of the width of the ribbon, the grain structure (Figure 2) is similar to the grain structure of ribbon grown for a full width melt (Figure 3).



Figure 1: Grain structure at the edge, rigid edge method

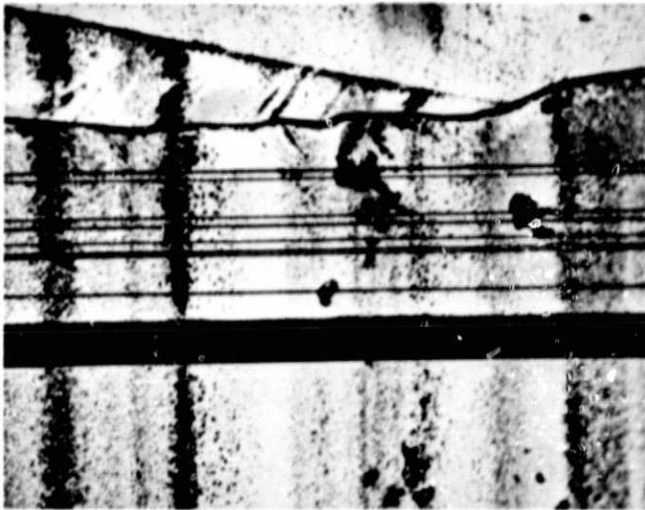


Figure 2: Grain structure at the center, rigid edge method

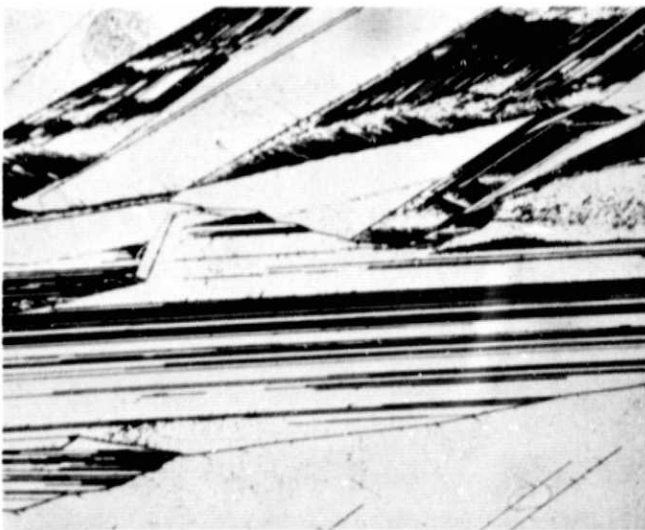


Figure 3: Grain structure, full width melt

We are seriously evaluating use of the "Rigid Edge" technique for achieving high production rates with the RTR method. The CVD ribbons would be grown with a constant limited length. The ribbon sections would be automatically loaded into a cassette, where they could be stored until they are ready for recrystallization. The RTR process would also feed the constant length ribbons into a cassette. In order for this method to be realizable, the full length of the ribbons must be utilized. This would not be possible with the conventional RTR method, since the ribbons must be supported on both ends, implying a loss of  $\sim 15$  cm at each end. However, if the melt is prevented from actually reaching the edge of the ribbons, a thin unmelted strip  $\sim 1$  mm wide on each side of the ribbon can support the ribbon, even when it is held at one end only. Thus, the "Rigid Edge" technique allows all the ribbon, except for a strip  $\sim 1$  mm wide around the perimeter, to be recrystallized. Since the grain structure of this ribbon is very similar to that obtained with the conventional RTR method, it is expected that comparable efficiencies will be maintained.

Consider a constant length ribbon 3 inches wide and 2 feet long. If 1 mm along each edge is lost because of rigid edge processing, the material use efficiency is 97%. The potential advantages of rigid edge growth far outweigh this small loss and, considering that solar cell processing required removal of some material along the substrate periphery, the relative loss of material, compared to current practice, should be well under 3%.

A 3" x 24" solar cell at 12% efficiency will generate 6 watts. Thirty-four of these cells in a package slightly larger than 4 feet square would generate over 200 watts. The constant length ribbon would permit designing all equipment for the entire process sequence to handle the same size substrates. This may be accomplished using cassettes similar to those presently in use for processing

Czochralski wafers, so a transition from Cz to ribbon technology can be smoothly affected. Also, since the ribbon will be only 100  $\mu\text{m}$  thick, occasional breakage will occur; standardization on a constant size of substrate will permit easy recovery of an automated process, and less loss of material after breakage.

## 2.0 POLYCRYSTALLINE RIBBON DEVELOPMENT

We have had some difficulty in reproducing our recent success in growing long polycrystalline silicon ribbons. The main problem appears to be a Venturi effect at the end seals of the CVD furnace. At the entrance seal, the change from the stainless steel block to the fiberglass curtain was counterproductive. The incoming  $\text{H}_2/\text{SiHCl}_3$  gases tend to suck air in through the furnace. At the exit, a similar effect is occurring with the suction induced by the hydrogen burn-off at the exhaust. In our original successful deposition, this exhaust had been almost totally blocked by  $\text{SiO}_2$  deposits. This forced some gases out into the room, and this outward gas flow effectively prevented air from leaking into the reaction chamber.

Several modifications were made to the furnace entrance in attempting to prevent air from entering the reaction tube. It was found that the O-ring seals around the quartz tube were unreliable. When tightened sufficiently to make a seal, they often broke the quartz reaction tube. When the tube did not break, a defective seal resulted in  $\text{SiO}_2$  formation.

Figure (4) shows the present configuration of the entrance. Process gases are now injected inside the quartz tube rather than through the center block. A seal plate, with a narrow slot to admit the Mo substrates has been added. A fiberglass curtain on the furnace side helps to reflect the radiant energy, and a slitted Viton curtain makes a tight seal. The O-ring seals around the quartz

ORIGINAL PAGE IS  
OF POOR QUALITY

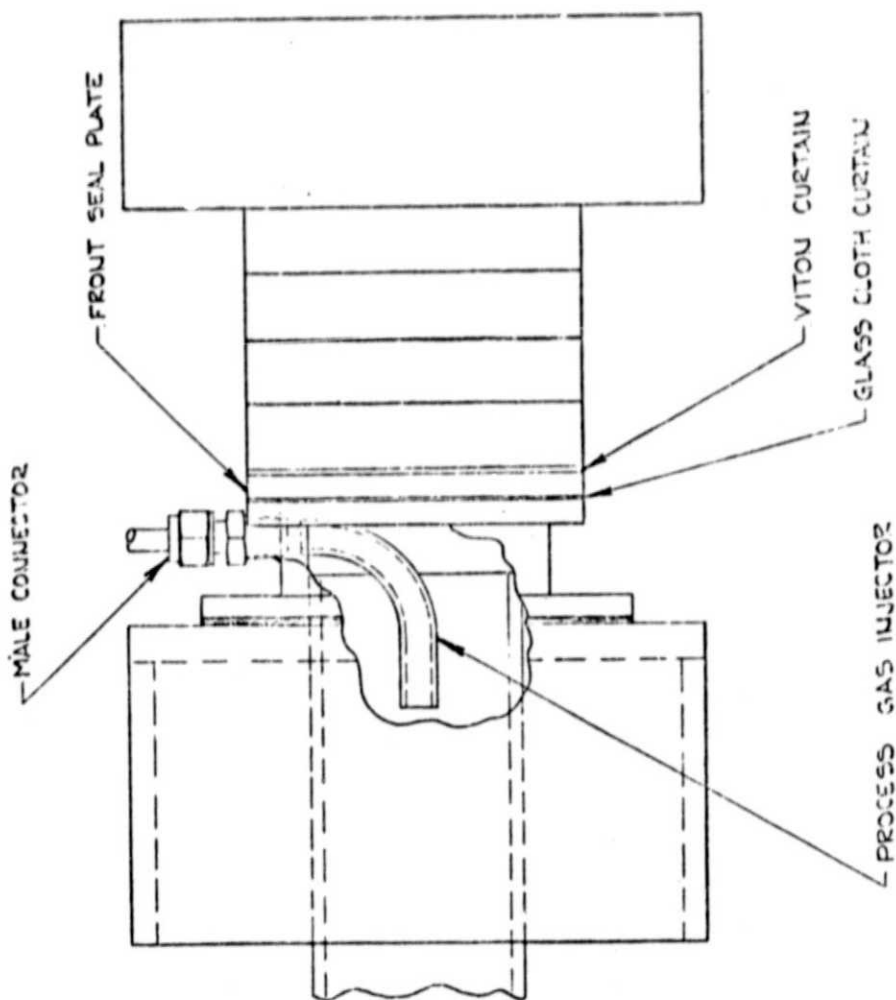


Figure 4: Entrance Seal, CVD Furnace

UNLESS OTHERWISE SPECIFIED, TOLERANCES: INCHES .XX ± .001 .XXX ± .0005 MILLIMETERS .XX ± .005 .XXX ± .0025 ANGULAR ± .5°		MATERIAL HEAT TREAT FINISH	MOTOROLA INC. Electronic Semiconductor Division
CHECK ALL DIMENSIONS FROM THE CENTERLINE UNLESS OTHERWISE SPECIFIED UNLESS OTHERWISE SPECIFIED, DIMENSIONS ARE TO BE TAKEN FROM THE CENTERLINE UNLESS OTHERWISE SPECIFIED, DIMENSIONS ARE TO BE TAKEN FROM THE SURFACE		TITLE CVD ENTRANCE SEAL ASSEMBLY MODIFICATIONS	PART NO. 04713 DRAWING NO.
DATE: 10/11/67 BY: J. J. BROWN CHECKED: J. J. BROWN APPROVED: J. J. BROWN		DATE: 10/11/67 BY: J. J. BROWN CHECKED: J. J. BROWN APPROVED: J. J. BROWN	DATE: 10/11/67 BY: J. J. BROWN CHECKED: J. J. BROWN APPROVED: J. J. BROWN

have been eliminated. Instead, RTV silicone is used to seal the metal parts to the quartz tube. These modifications have proved successful.

In the latest run a ribbon 140 cm long sheared off from a 150 cm x 5 cm substrate. Unfortunately the shearing took place in two sections, inside the furnace, indicating that a different temperature profile may be required for shearing to take place in long ribbons without periodic breaking of the ribbon. The longer ribbon of the two pieces was 85 cm x 5 cm.

## 2.1 SUBSTRATE STUDIES - MULTILAYER SYSTEMS

Multilayer substrate systems are conceptually a promising approach for reducing the Mo concentration in the silicon ribbon deposited on them by CVD. The general approach to a multilayer substrate is to have a diffusion barrier between the Mo base and the polycrystalline silicon ribbon. The two most obvious materials for use as a diffusion barrier are  $\text{Si}_3\text{N}_4$  and  $\text{SiO}_2$ , since neither would introduce a new element into the system. Experiments with  $\text{Si}_3\text{N}_4$  layers eventually proved to be disappointing, the silicon nitride film being converted to  $\text{MoSi}_2$  in the presence of hydrogen and the chlorosilanes. This results in the remaining unconsumed  $\text{Si}_3\text{N}_4$  separating from the  $\text{MoSi}_2$  layer and the silicon ribbon thus removes the  $\text{Si}_3\text{N}_4$ . Neutron activation analysis analyses (discussed in Section 3.0) confirm that only the first deposition results in a much lower molybdenum level. Thus, for the diffusion barrier properties of the  $\text{Si}_3\text{N}_4$  to be effectively utilized, it would require re-coating after every deposition.  $\text{SiO}_2$ , however, has shown continued promise.

In order to use the TESS technique successfully, a  $\text{MoSi}_2$  layer must be formed. Consequently, we have pursued two approaches. The simplest method is to deposit 1 micron of Si, 0.1 microns of  $\text{SiO}_2$  and then the CVD ribbon on the Mo substrate.

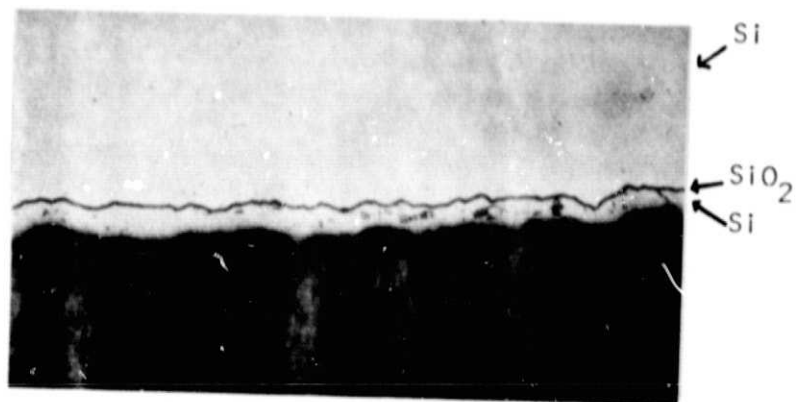
The ribbons sheared at the MoSi<sub>2</sub>-Si interface. They were then etched to remove the 1 micron Si layer, and the SiO<sub>2</sub>. Figure 5 is a micrograph of a ribbon (before etching) showing the two Si layers sandwiching the SiO<sub>2</sub> diffusion barrier. This technique has two advantages over our present method of etching about 20 microns from the silicon ribbon surface which was in contact with the Mo substrate: it reduces the etching of the silicon by 95% and it should produce an even higher purity Si ribbon.

The second method uses a thin (5,000 Å) molybdenum layer sputtered on top of the 1 micron-thick silicon dioxide diffusion barrier deposited on top of the Mo substrate. The ribbons sheared in normal fashion, leaving MoSi<sub>2</sub> film on the oxide layer. Should this technique be shown to be totally successful, a very significant improvement in substrate recycling may be expected, since the substrate is completely protected from the silicon. A cross-section is being made of the substrate and the ribbon. An additional virtue of the sputtered Mo adjacent to the depositing Si surface is the high purity of the sputtered layer, compared to metallurgical grade Mo. Silicon ribbons prepared by these methods are being evaluated by neutron activation analysis.

### 3.0 NEUTRON ACTIVATION ANALYSIS

The results of neutron activation analysis for Mo are shown in Table 1. The best results were obtained for samples 513 and 242BR, in which Mo could not be detected.

Sample 513 was grown by using a 0.1 μm thick SiO<sub>2</sub> layer as a diffusion barrier on top of a thin Si layer deposited on the Mo substrate. This method has two advantages over our present method. It produces a ribbon with the lowest Mo impurity level (since the SiO<sub>2</sub> has proven to be an excellent diffusion barrier) and it will reduce the total silicon lost by etching, since the total thickness



Magnification : 200 X

SiO<sub>2</sub> Diffusion Barrier- Cross-Section.



of the Si and SiO<sub>2</sub> layers is  $\sim 1 \mu\text{m}$ , while we typically remove about 20  $\mu\text{m}$  with our present method. Sample 242 is an RTR ribbon regrown from etched CVD feedstock, included on this list for comparative purposes.

Sample 536, grown using molybdenum-oxide-molybdenum layers, was not quite as successful. Sample 513, which was grown in the semicontinuous system, shows an Mo level  $\sim 0.1$  ppm. This result is promising, since only 10  $\mu\text{m}$  were removed from this sample.

Sample 481 (which was not etched) was grown from a SiH<sub>4</sub> source. Since Cl was eliminated from the system - thus eliminating the possibility of a molybdenum chloride autodoping mechanism - this experiment confirms that the main contamination mechanism is likely to be solid state diffusion, probably along the grain boundaries of the CVD ribbon.

The samples identified as SNA1 - SNC2 were ribbons deposited on silicon nitride coated Mo substrates. The letter in the I.D. denotes a particular Mo substrate, while the number denotes whether this ribbon was the first, second or third grown on that substrate. These results show that although the silicon nitride effectively reduces Mo contamination for the first deposition, it is ineffective for subsequent depositions. Thus, in order to use the silicon nitride layers as a diffusion barrier, we would have to coat the substrates prior to each deposition.

#### 4.0 DIFFUSION LENGTH MEASUREMENTS BY SPV, OCPV

We have recently reported some very long diffusion lengths in RTR silicon, including many values over 200 microns after gettering. It is possible that some of these very high values are anomalous, i.e. they do not reflect the true quality of the material.

TABLE I  
NEUTRON ACTIVATION ANALYSIS

<u>Sample I.D.</u>	<u>Mo Concentration (ppma)</u>	<u>Sample Description</u>
536	0.13	Mo (substrate) - SiO <sub>2</sub> - Mo (5000 Å sputtered layer) - Si ribbon. Sample etched after deposition.
513	N.D. < 0.04	Si - SiO <sub>2</sub> - silicon ribbon. Sample etched after deposition.
242BR	N.D. < 0.15	Regrown silicon ribbon. Feedstock etched after deposition.
R13	0.12	Silicon ribbon grown in semi-continuous system, etched 30 seconds.
481	30	Silicon ribbon grown from SiH <sub>4</sub> (not etched).
SNA1	0.17	First Deposition.
SNA2	8.1	Second Deposition.
SNA3	3.5	Third Deposition.
SNB1	0.15	First Deposition.
SNC1	0.3	First Deposition.
SNC2	21.0	Second Deposition.

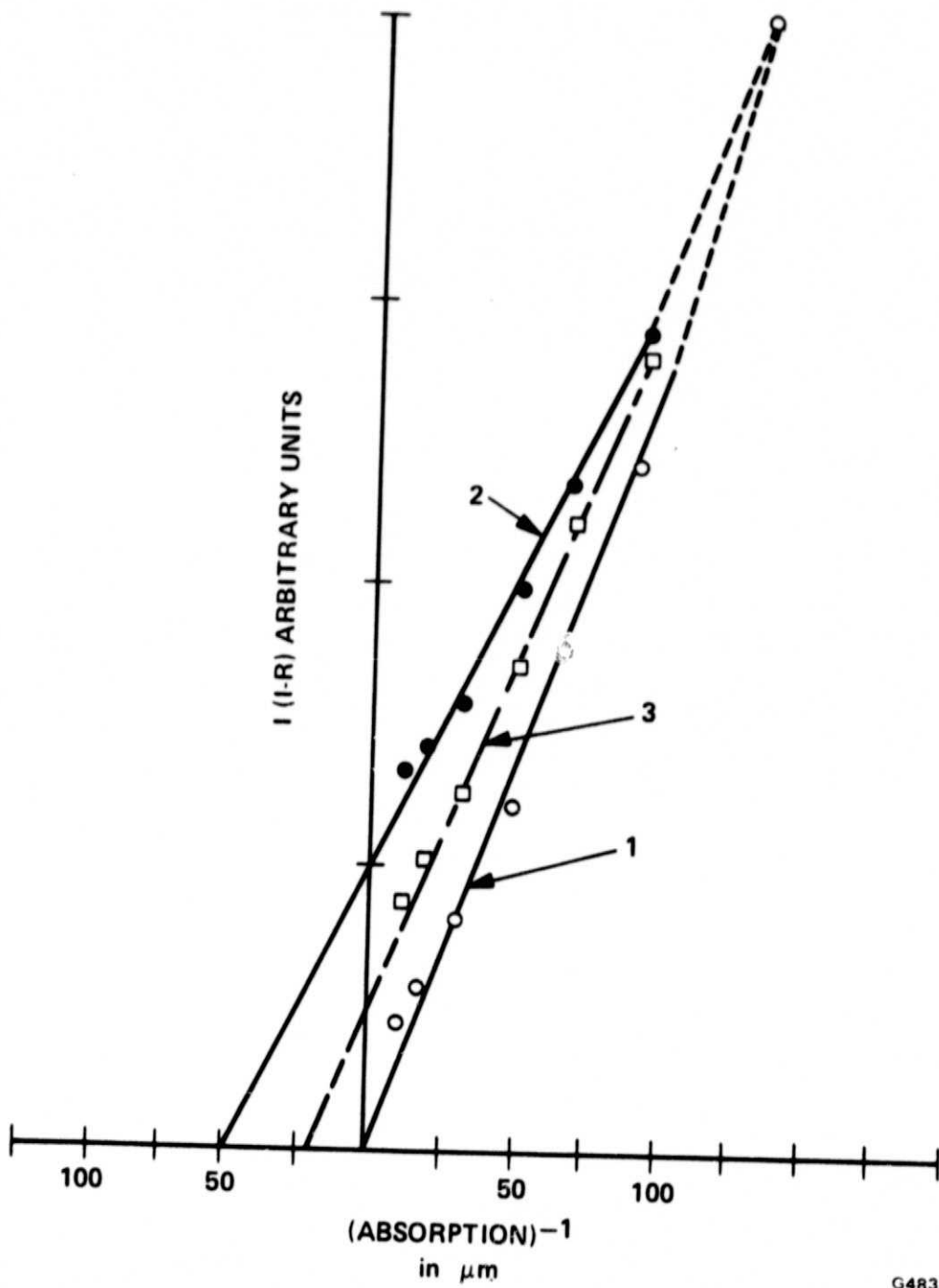
A brief experiment has shown that the measured diffusion length can be light intensity dependent. In a typical case, an increase in the light intensity by a factor of 5 reduced the apparent diffusion length from 200 microns to 70 microns. Further increases in light intensity did not further reduce the diffusion length. We should emphasize that this effect was found to apply only to some samples with very long apparent diffusion lengths. The diffusion lengths we have reported in the range 5 - 100 microns are still considered reliable.

For silicon ribbon with varying diffusion length but homogeneous in other material properties, the measured diffusion length would "average" out the good and bad areas. Such an experiment was carried out using two cells (see Figure 6). Curve #1 was obtained on an essentially zero diffusion length cell, and curve #2 on a 50 micron diffusion length cell. The average value of the diffusion length would then be given by:

$$\bar{L} = k (L_1 A_1 + L_2 A_2) \cdot A^{-1}$$

where  $\bar{L}$  represents the average value for the two cells;  $L_1, A_1$  are the diffusion lengths and the areas, respectively of the cells ( $i = 1, 2$ ).  $A = A_1 + A_2$  is the total area, and  $k$  is a constant determined by the experimental conditions (1). Curve #3 was obtained by measuring the total response from both cells illuminated simultaneously. Thus the diffusion length measured by curve #3 falls between the values measured on individual cells, shown in curves #1 and #2.

In some cases, however, material inhomogeneities can lead to measured values of the diffusion length larger than the true value. A similar situation near a grain boundary has been discussed by Matare (2). Internal fields, possibly due to impurity distribution, grain boundaries or other defects produce an additional voltage with a wavelength dependence, thus affecting the apparent value of the diffusion length.



G483

Figure 6 : Diffusion Length Measurements on Inhomogeneous Material.

## 5.0 SOLAR CELLS ON GETTERED SILICON RIBBONS

Another lot of solar cells fabricated on RTR silicon grown from pre-etched CVD feedstock has been evaluated. Two preliminary  $\text{PH}_3$  gettering steps were used to improve the diffusion length. These ribbons were grown at 0.3"/minute, without an annealing furnace. The cell size was 1 x 2 cm. The cells were defined by a mesa pattern, resulting in passivated junction edges.

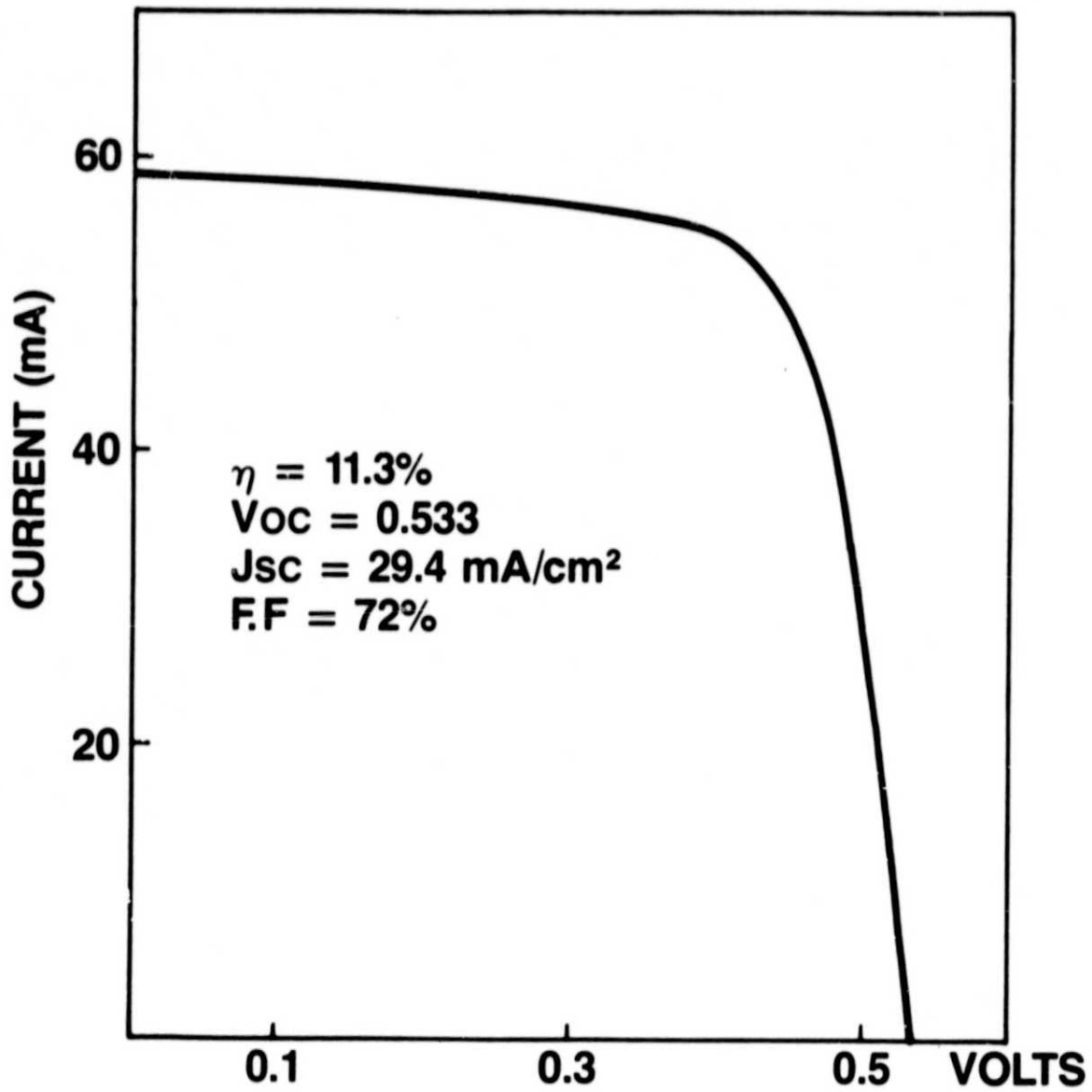
The average efficiency for this lot was 9.1%. The best cell (see Figure 7) had an efficiency of 11.3%, with  $V_{oc} = 0.533$ ,  $J_{sc} = 29.4 \text{ ma/cm}^2$  and a fill factor of 72%. One ribbon, 967R, contained 3 cells, all over 10%.

### 5.1 METALLIZATION SHADOWING

Although this lot of cells exhibited improved performance over previous lots, we did have a problem with pinholes in the  $\text{Si}_3\text{N}_4$  coating. This allowed metal to plate onto the exposed  $n^+$  surface layer, reducing the active area. Since the pinholes vary in size and density, it is difficult to estimate the degree of shadowing caused by this problem, but it may range up to 10%. For example, the shadowing on the 11.3% cell was estimated at about 1.7%. Presumably, based only on the increase in short circuit current, that cell could have reached an 11.5% efficiency.

### 5.2 VARIATION IN SHORT-CIRCUIT CURRENT

Considerable scatter has been observed in the measured values of  $J_{sc}$  for the "regrown from CVD" solar cells. The major cause for this variation has not yet been determined, but two factors can be identified. The first is a fluctuation in substrate resistivity (0.5 to 2 ohm-cm). This is due to the fact we are using two different reactors for the polycrystalline ribbon growth. One has consistently been producing a lower boron doping level than the other.



G637

FIGURE 7: I-V Curve High Efficiency Cell

TABLE II

RTR CELLS FABRICATED ON PRE-ETCHED CVD FEEDSTOCK

<u>Cell</u>	$\frac{V_{oc}}{\text{(Volts)}}$	$\frac{J_{sc}}{\text{(ma/cm}^2\text{)}}$	<u>Fill Factor</u>	<u>L (microns)</u>	<u>Efficiency</u>
967A-1	0.565	28.5	62%		10.0%
967A-2	0.562	28.6	65%		10.5%
967G-1	0.568	27.2	52%	57	8.0%
967S-2	0.520	24.3	57%	51	7.2%
982G-1	0.520	23.9	71%	27	8.8%
982G-2	0.535	24.9	53%	49	7.1%
982H-3	0.520	23.8	73%	38	9.0%
982H-4	0.513	21.7	73%	37	8.1%
982J-1	0.523	25.5	69%	24	9.2%
982K-2	0.525	24.9	69%	35	9.0%

A new boron source is being connected to the lower boron-doping furnace in order to correct this problem.

The second factor which is under investigation is the wide range of diffusion lengths observed in ribbons after gettering, and the correlation (or lack of it) with  $J_{sc}$ . Figure 8 is a plot of  $J_{sc}$  vs.  $L$  for all the pre-etched CVD cells in Table II. The diffusion lengths were measured by the OCPV method on completed cells, and  $J_{sc}$  is taken at  $100 \text{ mw/cm}^2$ . If there were excellent correlation, the variation in  $J_{sc}$  from cell to cell could be blamed on the variation in diffusion length over the ribbon. This variation could then be ascribed to grain size, dislocation densities or growth conditions. The lack of correlation evident in Figure 8 makes interpretation of the  $J_{sc}$  variation more difficult. The fault may lie in the way the OCPV method is used, since only a small area is measured.

### 5.3 METALLIZATION SINTERING

We have speculated whether the  $300^\circ\text{C}$  sintering of the metallization used on ribbon cells may have been responsible for the degradation observed in OCPV-measured diffusion lengths after gettering. It has now been shown that this  $300^\circ\text{C}$  step does not affect the diffusion lengths in RTR silicon. A CVD ribbon was placed in a  $300^\circ\text{C}$  furnace for sixteen hours prior to metallization, with no change in diffusion length. The cell listed in Table II as 967G was fabricated on this ribbon; it has an above average  $J_{sc}$ .

### 5.4 CELLS ON RIBBONS GROWN IN THE PURGEABLE FURNACE

A recent lot of solar cells has been made on ribbons grown in the purgeable furnace. The ribbons were grown in the rigid edge mode at  $1"/\text{min}$ . The lot is not yet fully characterized, but the best cell had an efficiency of 10.8% under



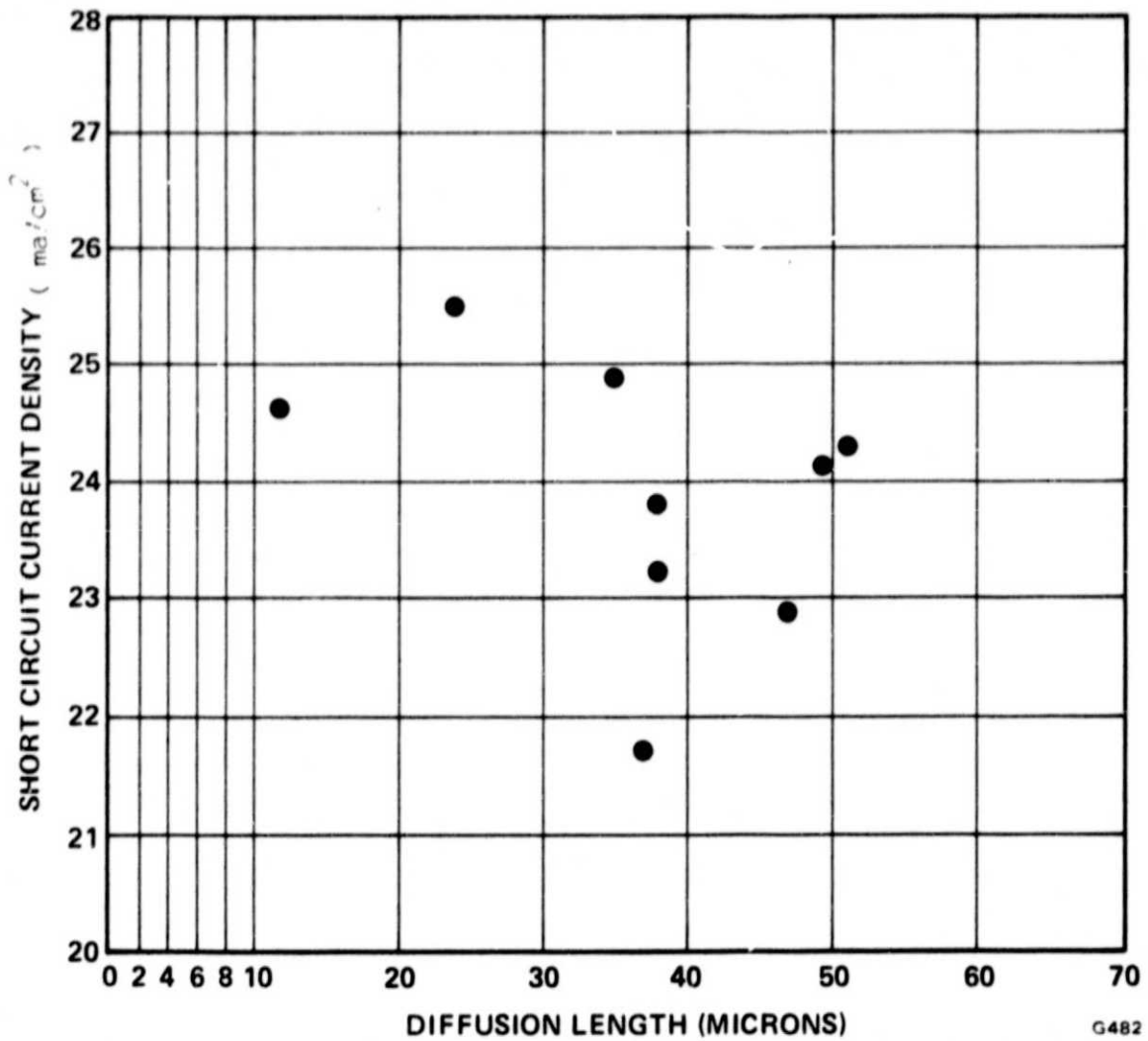


Figure 8: Correlation of Short-Circuit Current Density and Diffusion Length.

AM1 illumination. It had a short circuit current of  $26 \text{ mA/cm}^2$ , indicating a reasonably good diffusion length, its  $V_{oc}$  was .557 volts, and it had a very respectable fill factor of 75%. This lot of ribbons was all nominally  $.4 \Omega\text{-cm}$ , which accounts for the higher open circuit voltages. The actual resistivity has not yet been measured, however. The ribbons were not subjected to any repeated gettering steps as were the ribbons listed in Table II. The normal one step (2 sided)  $\text{PH}_3$  diffusion,  $\text{Si}_3\text{N}_4$  deposition, and sintered metallization mesa process was used.

### 5.5 LARGE AREA SOLAR CELLS

Using the purgeable furnace, CVD ribbons of 2 inch width were grown in the rigid edge mode. These were then processed so as to fabricate solar cells of dimensions  $2 \times 4$ ,  $2 \times 6$ , and  $4 \times 6$  cm. All of the cells have completed metal pattern etching of the  $\text{Si}_3\text{N}_4$  and are now being metallized. Figure 9 is a photograph of the metal pattern being used for the  $6 \times 4 \text{ cm}^2$  cell.

### 6.0 PRELIMINARY RESULTS OF INFRARED ABSORPTION MEASUREMENTS

Measurements of minority carrier diffusion lengths in RTR silicon have shown large increases following certain gettering/annealing process steps. It is necessary to know if this is due to impurity removal, reaction, or redistribution. Infrared absorption spectroscopy can be used to determine the concentration and/or chemical structure of some impurities. One impurity which is easily detected in silicon using I.R. spectroscopy is oxygen. The Si-O bond is detectable as a  $9.1 \mu\text{m}$  absorption peak.

Oxygen can be incorporated in RTR ribbon either by being included in the feedstock ribbon (e.g. when Czochralski silicon is used as the feedstock) or by

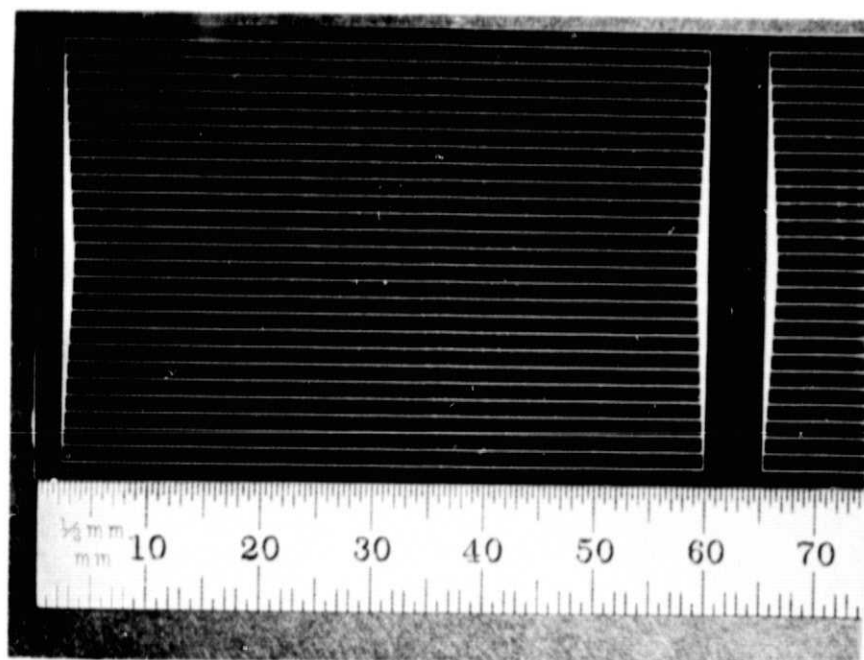


Figure 9:  $6 \times 4 \text{ cm}^2$  Cell

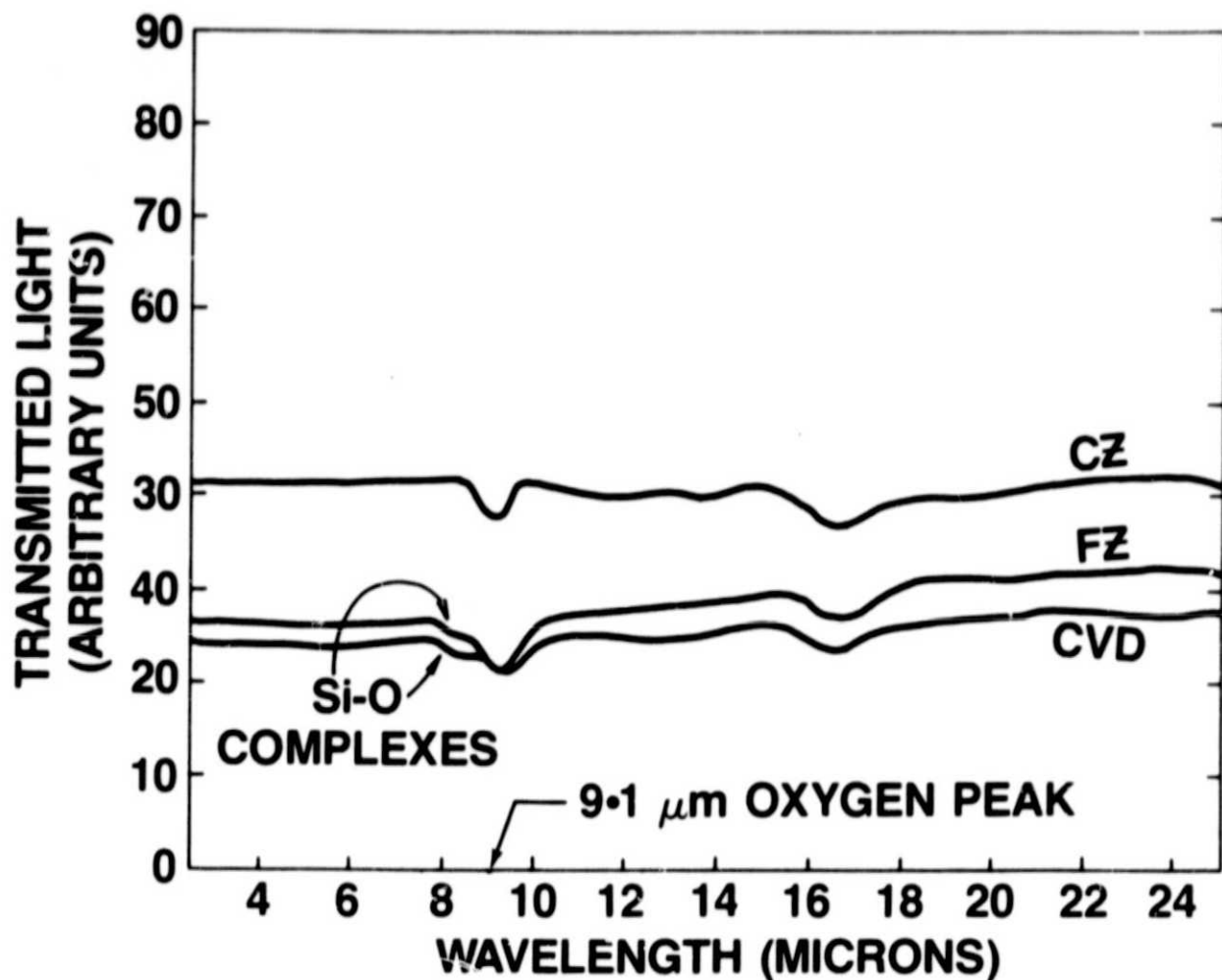
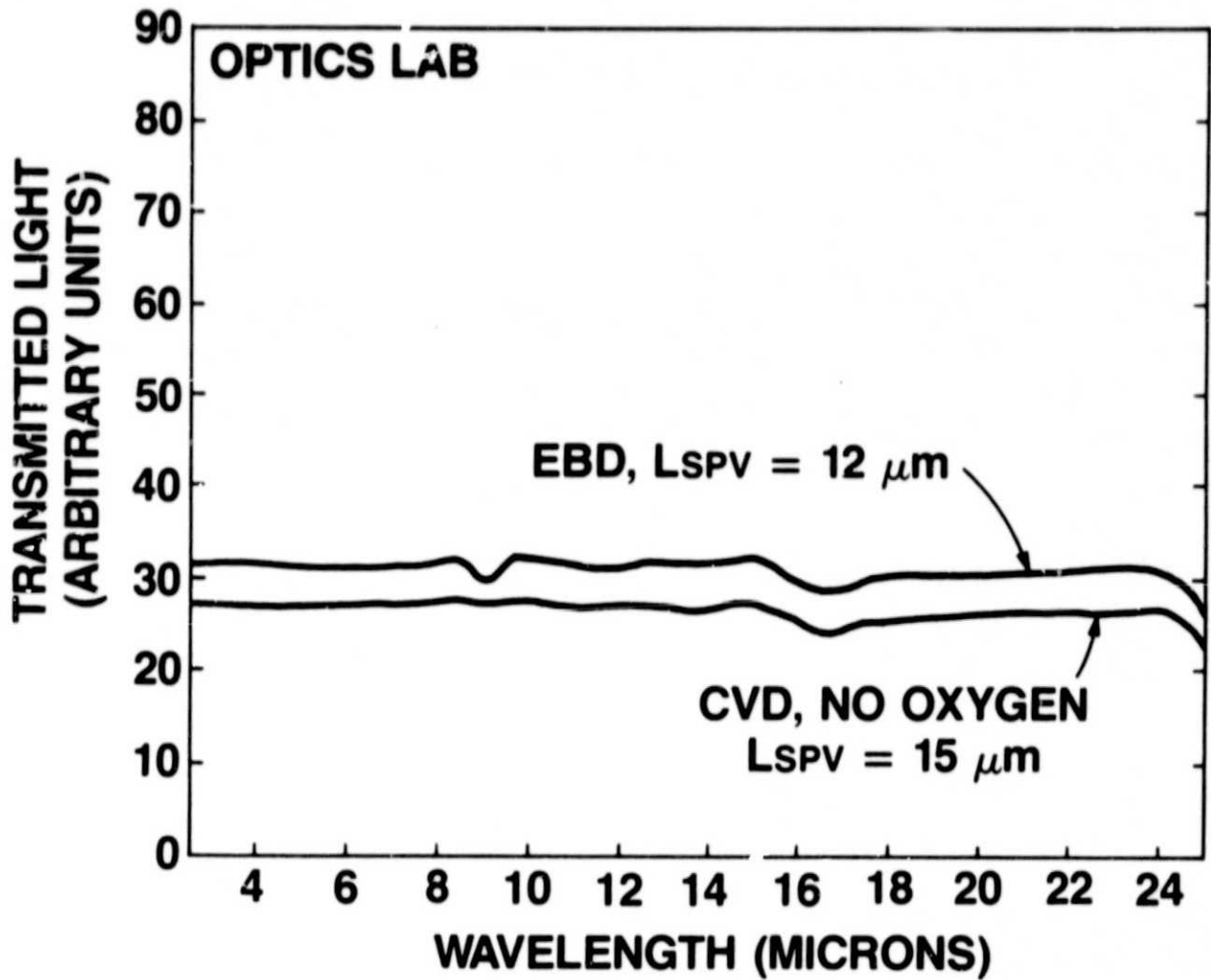


Figure 10: Behavior of Oxygen in RTR Silicon Ribbons Grown from Various Feedstock Types.



G640

Figure 11: Dependence of I on Net Oxygen and Oxygen Complexes

being present in the ambient atmosphere during growth. Most of our ribbon growths are carried out in a chamber which is too large for total ambient control. However, we have built a quartz enclosure (with ZnSe windows) which can be used for that purpose. Thus we can study low oxygen content ribbons grown from CVD feedstock in the quartz enclosure as well as ribbons grown from Czochralski feedstock (which have high initial oxygen concentrations) without the quartz enclosure.

The oxygen content is determined using an I.R. Fourier Transform Spectrometer. Typical transmission spectra are shown in Figures 10 and 11. The presence of oxygen is indicated by the absorption structure near  $9.1 \mu\text{m}$ . Figure 10 illustrates transmission spectra for ribbons grown from various types of feedstock. Oxygen is detected in all of the samples shown. Two samples indicate further absorption structure in the  $8.5 \mu\text{m}$  region, which usually indicates the formation of Si-O complexes. Figure 11 illustrates the difference between a sample grown in the well-purged quartz enclosure and conventionally grown ribbon. The sample grown in the quartz enclosure exhibits no detectable oxygen. Diffusion length measurements made on these samples by the SPV technique were virtually identical ( $\sim 12 \mu\text{m}$  as-grown) thus giving a preliminary indication that oxygen complexes/precipitates are not detrimental to ribbon minority carrier lifetime. Perhaps these results indicate oxygen complex segregation to grain boundaries or other defects.

## 7.0 PROBLEMS

We have solved the problem of quartz tube breakage in the CVD system. We must now work on achieving consistent separation for large area polyribbons.

## 8.0 PLANS

Fabricate a number of large area cells; attempt to achieve higher area growth rates, possibly by using multiple ribbons.

## 9.0 NEW TECHNOLOGY

The following New Technology Items have been developed on this program:

1. Description - Polygan Scanner System

Innovator - Dr. Richard Gurtler

Progress Reports - Technical Progress Report No. 14, October 1977,  
Pages 1, 10, 11A and 11

2. Description - Hemispherical Reflector to Improve Effective Absorption  
Coefficient of Liquid Silicon

Innovator - Dr. Richard Gurtler

Progress Reports - Technical Progress Report No. 7, Motorola Report  
2256/9, January 1, 1978 - March 31, 1978,  
Pages - Appendix Pages 11 to 13

3. Description - Dendritic Growth on RTR Silicon

Innovators - Dr. A. Baghdadi, R. J. Ellis, Dr. R. W. Gurtler

Progress Reports - Technical Quarterly Report No. 6, Motorola Report  
No. 2256/8, October 10, 1977 - December 31, 1977,  
Pages - 14 to 23

4. Description - Controlled Dendritic Growth

Innovators: Dr. A. Baghdadi and R. J. Ellis

Progress Reports - Monthly Report No. 21, August 1978, JPL/DOE No. 954376,  
Page 1

5. Description - Coated Substrates for Silicon Deposition

Innovator - Dr. R. Legge

Progress Reports - Monthly Report No. 20, July 1978, JPL/DOE No. 95476,

Page 20

10.0 PROGRAM MILESTONES

Activities associated with the total program are shown in the Milestone Chart contained in Appendix I.



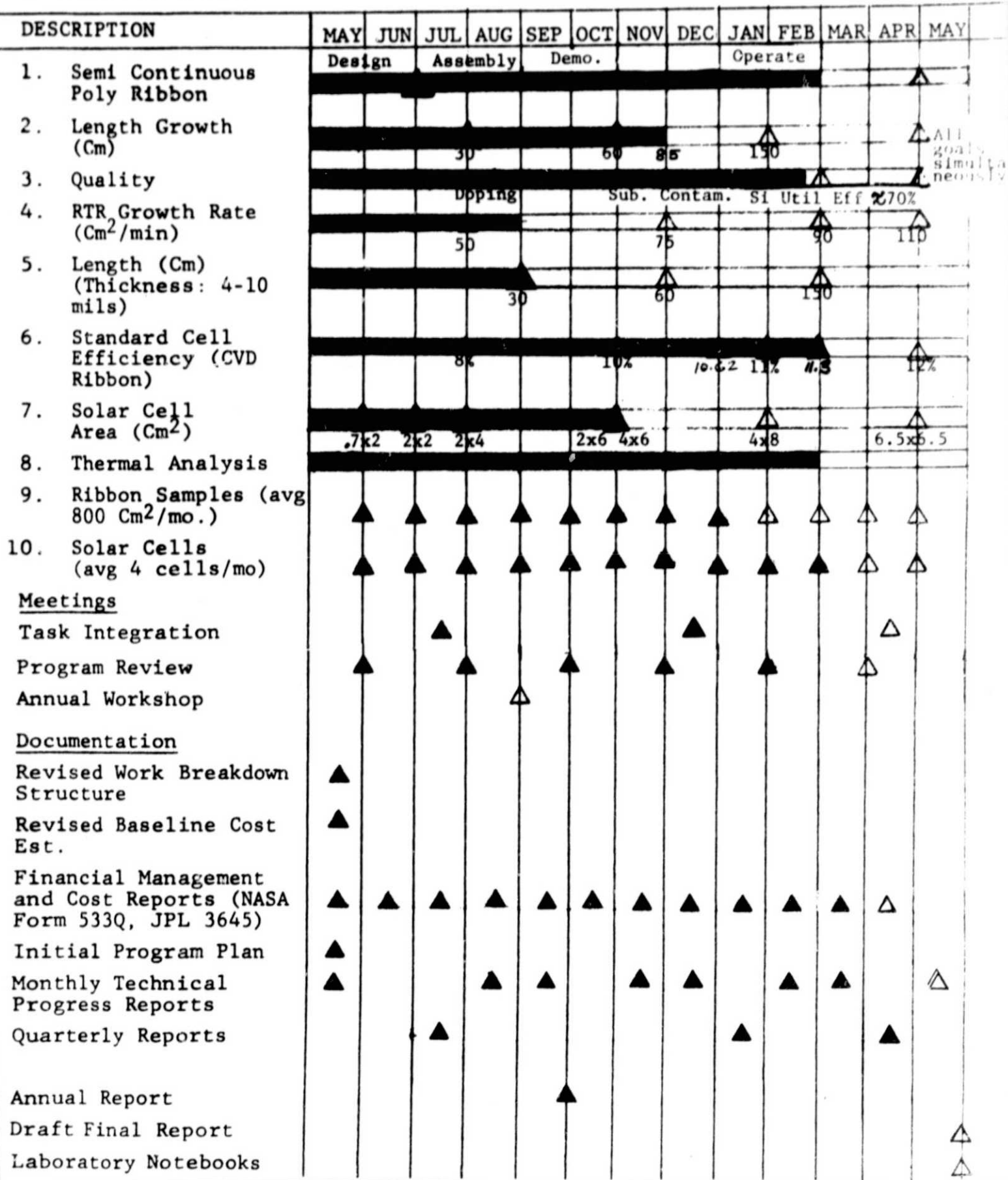
## REFERENCES

- (1) ASTM Annual Book of Standards, F391-73T, 1974.
- (2) H. F. Matare "Defects Electronics in Semiconductors". Wiley-Interscience, 1974.

# MILESTONE CHART

Contract No. 954376

MOTOROLA PROJECT NO. 2319-2325



All goals simultaneously

LEGEND  SCHEDULE  COMPLETED ▲ DELIVERY SCHEDULE  DELIVERED